

Fast Recession of a West Antarctic Glacier

E.J. Rignot¹

Satellite radar interferometry observations of Pine Island Glacier, in West Antarctica, reveal that the hinge-line position of this major ice stream retreated 1.2 ± 0.2 km per year between 1992 and 1996, which in turn implies ice thinning at 3.5 ± 0.6 m ice per year. The thinning trend is attributed to enhanced basal melting of the floating glacier tongue by warm ocean waters. If the fast retreat continues, it could trigger the wider-scale disintegration of the West Antarctic Ice Sheet.

Submitted to *Science*, April 6, 1998

Manuscript Number 98xxxx.

Received April, xx 1998

¹E.J. Rignot, Jet Propulsion Laboratory, California Institute of Technology, MS 300-235, Pasadena, CA 91109-8099, USA; E-mail: eric@adelie.jpl.nasa.gov; Ph. 818 354-1640

Pine Island Glacier, in West Antarctica, is a major ice stream which drains 172,000 km² of ice area into Pine Island Bay, in the Amundsen sea¹⁻⁶ (Fig. 1A). Two decades ago, T. J. Hughes^{5,6} highlighted this glacier as being most vulnerable to climate change and a possible trigger for the disintegration of the West Antarctic Ice Sheet. The ice stream flows rapidly, unrestrained by a large ice shelf at its junction with the ocean, over a bed substrate well below sea level which deepens inland. This flow configuration is inherently unstable^{7,8} because a retreat of its grounding line (where the glacier reaches the ocean and becomes afloat) would be self-perpetuating and irreversible, regardless of climate forcing.

Despite its theoretical interest, few data exist on Pine Island Glacier and no evidence of present-day retreat has been collected. Early estimates of its mass budget suggest massive ice thickening in this region^{2,3}. This view was recently challenged by an hydrographic survey of Pine Island Bay which revealed that the glacier experiences basal melt rates one order of magnitude larger than those recorded on large Antarctic ice shelves, thought to be the norm^{9,10}. High basal melting is apparently fueled by an influx of relatively warm ocean waters from the southern Pacific. Taking basal melting into account entails a major revision of the glacier mass budget. A pre-requisite to the revision is to know precisely where the glacier enters in contact with the ocean waters.

Here, we use satellite radar interferometry from the Earth Remote Sensing instruments, ERS-1 and 2, to detect the glacier grounding-line position and its eventual horizontal migration with time. A quadruple difference interferometry technique^{11,12} is employed to map the glacier hinge-line position (or limit of tidal flexing) for the first time, in great detail, across the entire glacier width¹³ (Fig. 1). Feature tracking applied on the same data procures detailed vector measurements of the glacier velocity¹⁴.

Combining this information with surface elevation from an altimetric digital elevation model of Antarctica¹⁵, we calculate an ice volume discharge at the hinge line¹⁶ of $76 \pm 4 \text{ km}^3 \text{ ice a}^{-1}$. The mass input to that region from mass accumulation in the interior¹⁷ is estimated at $71 \pm 7 \text{ km}^3 \text{ ice a}^{-1}$. If the numbers are correct, the glacier loses $5 \pm 5 \text{ km}^3 \text{ ice a}^{-1}$ to the ocean, which is close to equilibrium¹⁸.

Comparing quadruple difference radar interferograms acquired in 1992, 1994 and 1996 along both ascending and descending tracks of the satellites¹⁹, we also find that the hinge-line position of Pine Island Glacier retreats rapidly at a mean rate of $1.2 \pm 0.2 \text{ km a}^{-1}$ between 1992 and 1996 (Fig. 1B-F and 2A).

Hinge-line retreat may result from an increase in sea-level height, a decrease in ice thickness, or an increase of the height of the sea bed⁶⁻⁸. The latter factor is insignificant over the time scale considered here, while changes in sea level due to ocean tide should yield hinge-line migration of less than 1.3 km on this glacier²⁰. We therefore attribute the 1992-1996 hinge-line retreat to a decrease in glacier thickness. The corresponding rate of thinning is $3.5 \pm 0.6 \text{ m a}^{-1}$ at the hinge line.

Mass accumulation and sublimation at the surface of the glacier floating tongue are both known to be small (less than 1 m a^{-1}) and in balance^{1,21}. Thinning of the floating tongue is thus unlikely to be caused by a major change in its surface mass budget. Similarly, the glacier velocity has been stable at the 10% level since the 1970s^{1,4} and did not change by more than 1% between the 1992 and 1996 ERS interferograms²². The most likely explanation for the thinning trend is therefore that the basal melt rates eroding the glacier at its underside are too large to maintain the floating tongue in a state of mass balance.

Calculations of ice discharge seaward of the hinge line indicate that basal melting probably exceeds $50 \pm 10 \text{ m a}^{-1}$ in the first 20 km of the sub-ice cavity, subsequently decreasing to average $24 \pm 4 \text{ m a}^{-1}$ between the hinge line and the calving front (Fig. 3C).

The large melt rates recorded in the proximity of the hinge line imply that Pine Island Glacier is even more sensitive to ice-ocean interactions than inferred from the hydrographic survey conducted at the ice front⁹.

Application of a two-dimensional thermo-haline circulation model to the sub-ice cavity shows that basal melting is sensitive to even slight changes in ocean conditions¹⁰. An increase in sea-water temperature from +1.5°C to +2.0°C, for instance, would increase basal melting by 30%. Inter-decadal variations in ocean temperature of a few tenths of a degree have been reported for the deep water in the southeast Pacific²³. Hence, basal melting could easily increase by several meters per year in response to an increase in sea-water temperature, and trigger glacier thinning and retreat of Pine Island Glacier.

Sediment cores collected in Pine Island Bay show that a substantially more extensive ice shelf cover was present as recently as 100 years ago²⁴. Terminus locations recorded in 1966, 1973 and 1985 suggest a glacier retreat of 0.8 km a⁻¹. More recent satellite imagery indicates more stable ice front conditions^{1,4}, with periodic calving of massive icebergs complicating the definition of the ice front position (see Fig. 1A). The recent ice front stability contradicts the radar interferometry record which is unequivocal of a glacier hinge-line retreat at a mean rate of 1.2 km a⁻¹ and which also supports the presence of an extensive ice shelf in the recent past. Perhaps the ice-front evolution is controlled by other factors than those driving hinge-line retreat. Basal melting is lower at the ice front (Fig. 3C) as the glacier draft reaches shallower depths, hence ice thinning due to enhanced basal melting should be less there than up glacier. Furthermore, the current ice-front position is pinned down by numerous emerging islands or ice rises (Fig. 1A) which may temporarily slow down or halt the ice front retreat despite ice thinning. In contrast to the difficulty of observing significant changes in ice front position, pronounced glacier thinning occurring near the hinge

line has an immediate effect on its position because that position is governed by hydrostatic equilibrium of the ice. If this interpretation is valid, radar interferometry then provides a most unique and relevant record of present-day glacial retreat.

Whether the retreat of Pine Island Glacier is a unique phenomena in West Antarctica, or the signal of a wider-scale ice-sheet disintegration cannot be answered at present. Warm circumpolar deep water reaches other sectors of the continental shelf in the Amundsen and Bellinghausen seas besides Pine Island Bay, hence high basal melt rates and ice sheet retreat could develop in these regions as well^{1,9,10}.

REFERENCES AND NOTES

- 1 A. Jenkins, D. G. Vaughan, S. S. Jacobs, H. H. Hellmer, and J. R. Keys, *J. Glaciol.* **43**(143), 114-121 (1997).
- 2 D. Lindstrom and D. Tyler, *Antarct. J.* **19**(5), 53-55, (1984); D. Lindstrom and T. J. Hughes, *Antarct. J.* **19**(5), 56-58, (1984).
- 3 R. D. Crabtree and C. S. M. Doake, *Ann. Glaciol.* **3**, 65-70, (1982).
- 4 B. K. Lucchitta, C. E. Rosanova, and K. F. Mullins, *Ann. Glaciol.*, **21**, 277-283 (1995).
- 5 T. J. Hughes, *J. Glaciol.* **24**(90), 493-495 (1979); T. J. Hughes, *J. Glaciol.* **27**(97), 518-525, (1981); G. H. Denton and others, *J. Glaciol.* **24**(90), 495-496 (1979); C. S. Lingle and J. A. Clarke, *J. Glaciol.* **24**(90), 213-230 (1979); R. H. Thomas, *J. Glaciol.* **24**(90), 167-177 (1979).
- 6 M. Stuiver, G. H. Denton, T. J. Hughes and J. L. Fastook, *The last great ice sheets*, Denton, G.H. and T. J. Hughes, eds., (New York, etc., John Wiley and Sons), 319-346.

- 7 J. Weertman, *J. Glaciol.* **13**(67), 3-11, (1974); R. H. Thomas and C. R. Bentley, *Quat. Res.* **10**(2), 150-170 (1978); R. H. Thomas, T. J. O. Sanderson and K. E. Rose, *Nature* **277**(5695), 355-358 (1979).
- 8 R. H. Thomas, *Climate processes and climate sensitivity*, J. E. Hansen and T. Takahashi, eds., (Geophysical monograph 29, Maurice Ewing Series 5; Washington D.C., American Geophysical Union), 265-274.
- 9 S. S. Jacobs, H. H. Hellmer and A. Jenkins, *Geophys. Res. Lett.* **23**(9), 957-960, (1996).
- 10 H. H. Hellmer, S. S. Jacobs, and A. Jenkins, *Antarct. Res. Ser.* **75**, in press (1998).
- 11 E. Rignot, *J. Glaciol.* **42**(142), 476-485 (1996); E. Rignot, S. P. Gogineni, W. B. Krabill and S. Ekholm, *Science* **276** 934-937 (1997); E. Rignot, *Ann. Glaciol.* in press (1998); E. Rignot, *J. Glaciol.*, in press (1998).
- 12 To locate a glacier hinge line with ERS radar interferometry, we form the difference between two radar interferograms combining ERS data acquired 1 day apart for the 1996 data, 3 days apart for the 1994 data, and 6 days apart for 1992 data. Differencing eliminates information common to both interferograms, which is the steady and continuous creep deformation of the glacier. After differencing, we remove the signal associated with the glacier topography using an altimetric DEM of Antarctica¹⁵ at a 5-km spacing, interpolated to the 20-m spacing of the radar interferograms. The coarse spatial resolution of the DEM is sufficient to remove the mean glacier surface slope (less than 2%) from the interferograms. The resulting quadruple difference interferograms measure the glacier surface displacement along the radar line of sight in response to changes

in ocean tide (a vertical motion). To process 1992 and 1994 quadruple difference interferograms successfully, the radar scenes are first co-registered with sub-pixel precision to follow the glacier motion (which exceeds 20 m in 3 days), and the interferograms are generated at the highest spatial resolution prior to differencing.

- 13 The inward limit of glacier tidal flexing defines the hinge-line position. It is mapped automatically by fitting (in the least square sense) an elastic beam model of tidal flexure¹¹ through individual tidal displacement profiles extracted across the zone of tidal flexure in a direction perpendicular to the iso-contours of vertical displacement of the glacier. The mapping precision is highest (80 m) in areas of high signal to noise ratio, large tidal amplitude, and large radius of curvature of the hinge line (e.g. along the glacier center line). It worsens along the side margins where the signal is eventually lost because of the limited resolution of the ERS radar system. Discrete hinge-line positions for which the r.m.s. error of the model fit is greater than 5 mm are not considered reliable. Other positions deviate on average by ± 200 m from a mean hinge-line profile.
- 14 Velocity in the along- and cross-track directions is obtained by applying a precision feature tracking technique [R. Michel, PhD Thesis, Universite PARIS XI, Dec. 1997] on the ERS data. The precision of the along-track displacements, which are independent of tide, is 49 m a^{-1} for one-day pairs and 8 m a^{-1} for 6-day pairs. The across-track displacements are 5 times less precise (20-m pixels instead of 4-m pixels), and also contaminated by tide (3 m tidal signal versus 13 m glacial motion in 6 days along the radar line of sight). To increase the precision, we combine two independent estimates of the displacements for the 1992 and 1994 data. For the 1996 data, ice flux is calculated using profiles

perpendicular to the along-track direction.

- 15 J. Bamber and R. A. Bindschadler, *Ann. Glaciol.* **25**, in press, 1998.
- 16 Ice discharge is calculated as the sum across of the glacier width of the ice velocity normal to a glacier transverse profile multiplied by ice thickness. Ice thickness is deduced from hydrostatic equilibrium of the ice using mean-sea-level surface elevation from the altimetric DEM of Antarctica, a sea-water density⁸ $\rho_w = 1027.5 \text{ kg m}^{-3}$, and a depth-averaged density of ice¹ $\rho_i = 900 \text{ kg m}^{-3}$. The same calculation repeated with 1992, 1994 and 1996 data yields an ice flux of, respectively, 76.3, 75.1 and 77.1 $\text{km}^3 \text{ ice a}^{-1}$. The mean value is $76.1 \pm 4 \text{ km}^3 \text{ ice a}^{-1}$, with a 5% error associated mainly with uncertainties in ice thickness.
- 17 Mass accumulation is on a 100-km grid, from M. B. Giovinetto, pers. comm. (1998); M. B. Giovinetto and C. R. Bentley, *Antarct. J. U.S.* **20**(4), 6-13 (1985). The drainage basin of Pine Island Glacier was drawn on the computer using an altimetric DEM of Antarctica interpolated to a 500-m sample spacing. Starting at low elevation from the end points of the profile selected for calculation of the hinge-line ice discharge, we find an accumulation area of $159,044 \pm 997 \text{ km}^2$ ($\pm 500 \text{ m}$ uncertainty over a 1993-km long contour), which yields a mass accumulation of $65.0 \pm 7 \text{ km}^3 \text{ a}^{-1}$ water equivalent, or $70.8 \pm 7 \text{ km}^3 \text{ ice a}^{-1}$ using an ice density of 0.917 kg m^{-3} . The level of confidence of the gridded accumulation data over this region is 10%.
- 18 At the hinge line, we measure a mean glacier velocity $V = 1.98 \text{ km/yr}$, thickness $h = 1.2 \text{ km}$ and width $W = 32.9 \text{ km}$. Reference (3) underestimate ice discharge by a factor 3 by calculating it at the ice front with $V = 2.1 \text{ km/yr}$, $h = 0.5 \text{ km}$ and $W = 26 \text{ km}$. Reference (2) uses $V = 0.7 \text{ km/yr}$, $h = 1.56 \text{ km}$ and $W =$

26 km for a grounding-line position more than 20 km too far inland. Upstream input flux estimated by the same authors relies on less precise elevation data than provided by 1994 satellite altimetry to define the glacier drainage basin, and on mass accumulation not in gridded form.

19 Multi-year ERS data from ascending and descending tracks are registered independently to reference scenes acquired in 1996 (ERS-1 Orbit 23627 for ascending tracks, and ERS-1 Orbit 23616 for descending tracks) using the cross-correlation of the signal intensity over non-moving parts of the scene. The precision of registration is better than ± 40 m in the along- and cross-track directions. To register ascending and descending tracks together, topographic information is required. We therefore project all data onto a common polar stereographic grid at 50-m spacing using surface elevation from the altimetric DEM of Antarctica. The two geocoded reference scenes for ascending and descending tracks (acquired 1 day apart) are subsequently co-registered to within ± 50 m using the cross-correlation of the signal intensity over the entire area (glacial motion is less than 7 m per day). This final co-registration provides the framework for comparing ascending and descending data of any year with ± 60 m, which is two orders of magnitude less than the detected hinge-line migration.

20 Hinge-line positions migrate back and forth by \dot{x} with changes in sea level (tide) \dot{z} and changes in ice thickness \dot{h} according to

$$\dot{h} = (\rho_w/\rho_i)\dot{z} - [\alpha - \beta(1 - \rho_w/\rho_i)]\dot{x} \quad (1)$$

where $\dot{h} > 0$ for thickening, $\dot{x} > 0$ for hinge-line retreat, ρ_w is the sea-water density, ρ_i is the depth-averaged density of ice, and α and β are, respectively, the surface and basal slopes counted positive upwards⁶. We estimate $\alpha = -0.5\%$ and

$\beta = 1.1\%$ at the hinge line from surface elevation and ice thickness data acquired by the British Antarctic Survey in February 1981³. Uncertainty in positioning accuracy of these data prevents us from making a direct comparison with the hinge-line position in the ERS data¹. We assume that the 1981 grounding line was located where described in reference (8). Surface slope calculated from the DEM at the location of the 1994 hinge line is also -0.5% . Hinge-line migration due to tide only is numerically $\dot{x} = 332 \dot{z}$. With ocean tides less than 4 m (which is the largest differential tidal signal detected in our data set), we find \dot{x} less than 1.3 km. Hinge-line migration due to changes in ice thickness only is numerically $\dot{x} = -290.6 \dot{h}$. Hence, the $1.2 \pm 0.2 \text{ km a}^{-1}$ hinge-line retreat of Pine Island Glacier translates into a thinning rate $\dot{h} = 3.5 \pm 0.6 \text{ m ice a}^{-1}$.

- 21 T. B. Kellog, D. E. Kellog and T. J. Hughes, *Antarct. J. U.S.* **19**(5), 56-58 (1985).
- 22 Differencing of ERS data acquired along the same track in 1992 and 1996 shows no difference in ice velocity on grounded ice at the 1 percent level.
- 23 J. H. Swift, *Intern. WOCE Newsletter* **18**, 15-17 (1995).
- 24 T. B. Kellog and D. E. Kellog, *J. Geophys. Res.* **92**(B9), 8859-8864 (1987).
- 25 We thank the European Space Agency for providing ERS data, S. Jacobs, A. Jenkins and H. Hellmer for stimulating discussions about the glaciological interest of Pine Island Glacier, J. Bamber for providing an altimetric topographic model of Antarctica, D. Vaughan for providing the 1981 ice sounding radar data, G. Peltzer for assistance in preparation of the figures, M. Schmeltz and G. Buscarlet for assistance in the processing of radar interferograms, and C. Werner for providing a synthetic-aperture radar interferometric processor. The

work was carried out at the Jet Propulsion Laboratory, California Institute of Technology, under a contract with the Polar Research Program of the National Aeronautics and Space Administration.

FIGURE CAPTIONS

Fig. 1. Normalized tidal displacements of Pine Island Glacier, West Antarctica recorded with ERS differential interferometry and color coded from purple (grounded ice), to yellow (glacier flexure zone) and blue (ice-shelf ice in hydrostatic equilibrium with the ocean waters). Color tone is modulated by the radar brightness of the scene acquired by ERS-1 on January 21, 1996 (Orbit 23627, Frames 5589 and 5607) © ESA 1996. No interferometric data is available in areas colored dark green. The data projection is a 50-m polar stereographic grid. ERS is flying north in (A-C) (ascending track, heading -49° from N) and south in (D-F) (descending track, heading -128° from N), illuminating the scene from its right. The normalization factors of the tide from (B) to (F) correspond to a maximum tidal displacement of, respectively, 2.2 m, 4.0 m, 3.2 m, 2.7 m, and 0.9 m. The fast-moving portion of the glacier is revealed by flow line features conspicuous in the radar brightness image. The hinge-line position, retrieved from model fitting in the region of interest¹³, is shown as a black thin continuous line separating grounded (purple color) from floating ice (blue color). Its finger-shaped appearance in (B) - (F) indicates the presence of thicker ice at the glacier center than along its sides. In (A), locally grounded areas or ice rises (emerging islands covered with ice and snow) are revealed between the hinge line and the ice front. These ice rises buttress the ice-shelf flow and may help temporarily stabilize the current ice-front position. The white square in (A) delineates the area shown in (B) - (F). (B) shows the hinge-line position and tidal displacement recorded in 1996 (ERS-1/ERS-2 orbit pairs 23627/3954 and 24128/4455; Frame 5589). Profile A-B of Fig. 2A is represented by the thick, white line running across the hinge line. Tidal displacements recorded in January 1992 (ERS-1 orbits 2970, 3056 and 3142; Frame 5589) are shown in (C); (D) 1996 (ERS-1/ERS-2 orbit pairs 22614/2941 and 23616/3943; Frame 5211); (E)

March 1994 (ERS-1 orbits 13826, 13869, and 13912; Frame 5211); and (F) February 1992 (ERS-1 orbits 3260, 3346 and 3432; Frame 5211). Decimal years are indicated at the top of (B)-(F). Between (B) and (C), the hinge line retreats 5.0 ± 1.0 km in 3.78 a (annae) over a 275-m wide region at the glacier center, and 3.5 ± 1.8 km on average across the entire glacier width. The variability in hinge-line retreat across the glacier width presumably reflects spatial variations in surface and basal slopes²⁰. The retreat is less along the glacier side margins due to steeper slopes (-1.2% versus -0.5% at the center) for the same amount of thinning. The retreat between (D) and (E) is 1.2 ± 1.0 km in 1.76 a along the center line. Between (D) and (F), the retreat is 4.7 ± 0.9 km in 3.98 a.

Fig. 2. (A) Tidal displacement measured by ERS along profile A-B (see Fig. 1B for location) for the 1996.1 and 1992.1 data (Fig. 1B and C). The data noise level is 1-2 mm. The hinge-line position inferred from model fitting is indicated by an arrow of different color for each year. The magnitude of the 1996 differential displacement is 3 times less than for the 1992 data because the 1-day repeat cycle of 1996 data is closer to the natural periodicity of semi-diurnal and diurnal tides than the 6-day repeat cycle of 1992 data. (B) Retreat of the hinge-line position measured in a 250-m wide region along profile A-B. Error bars represent a 1.3-km uncertainty in hinge-line position due to unknown tide. The mean retreat rate along the glacier center is 1.2 ± 0.2 km a⁻¹. The smaller retreat rate in 1994-1996 could be due to larger tidal amplitudes in the 1994 data, an increase in basal slope as the glacier retreats or year-to-year variations in glacier thinning²⁰. (C) Ice volume flux of Pine Island Glacier at discrete locations between the hinge line (distance = 0) and the ice front (distance = 50 km), parallel to flow lines. Ice velocity is inferred from along-track feature tracking of the 1996 ERS data¹⁴. The cumulative glacier area calculated from the hinge line is shown in red. Net basal melting under steady-state conditions

is equal to the decrease in ice flux divided by the area. The pronounced decrease in ice flux in the first 15 km is due to basal melting in excess of 50 m a^{-1} . Net basal melting decreases downstream. Ice flux increases after km 30 due to additional ice input from the south.

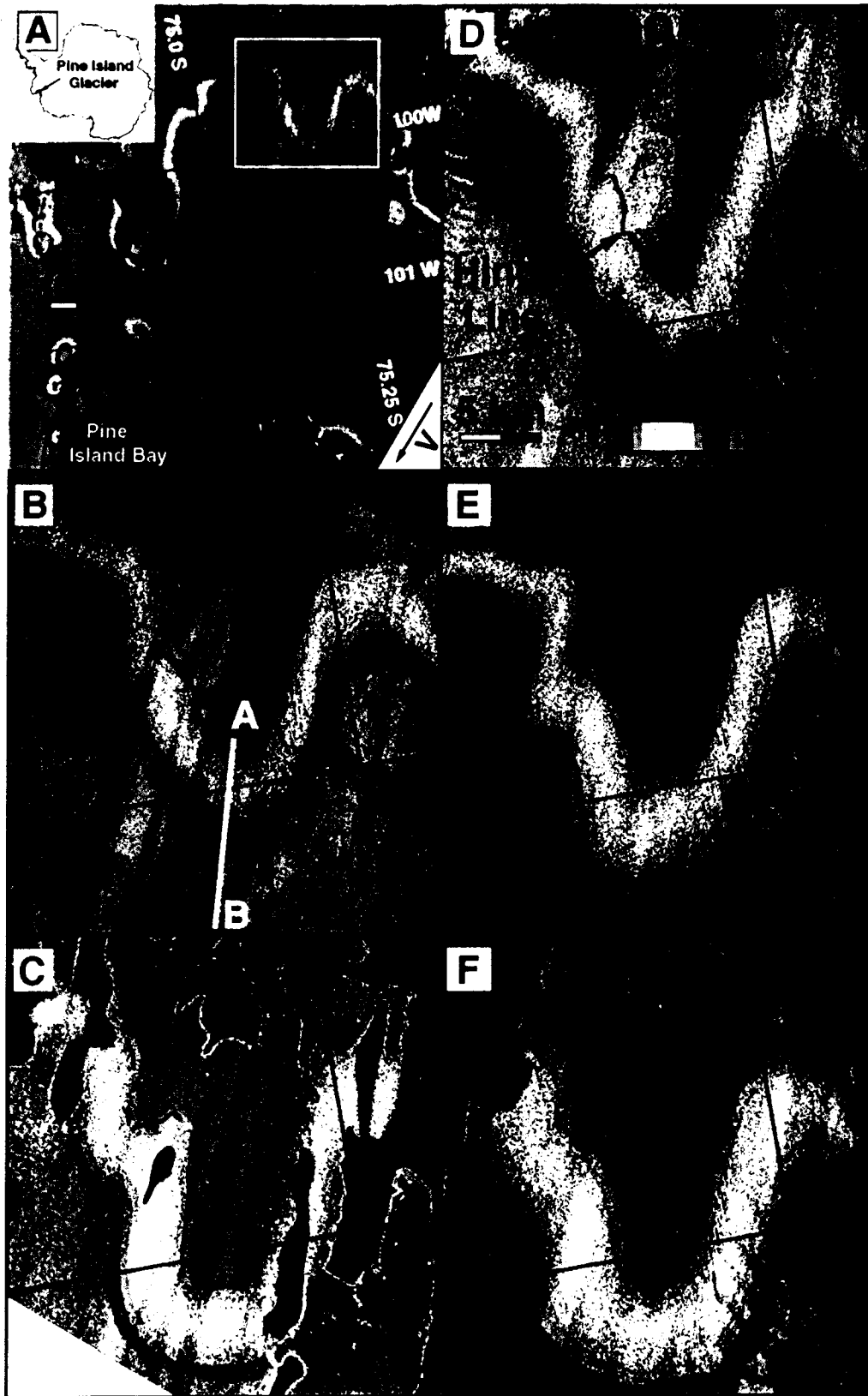


Fig. 1, Rignot

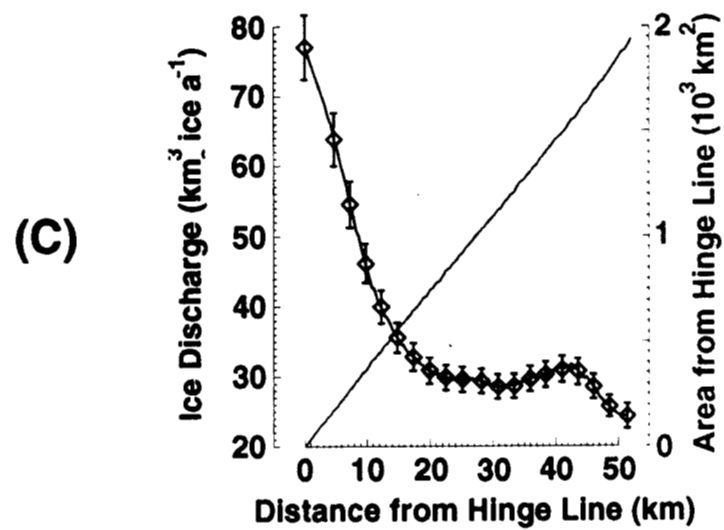
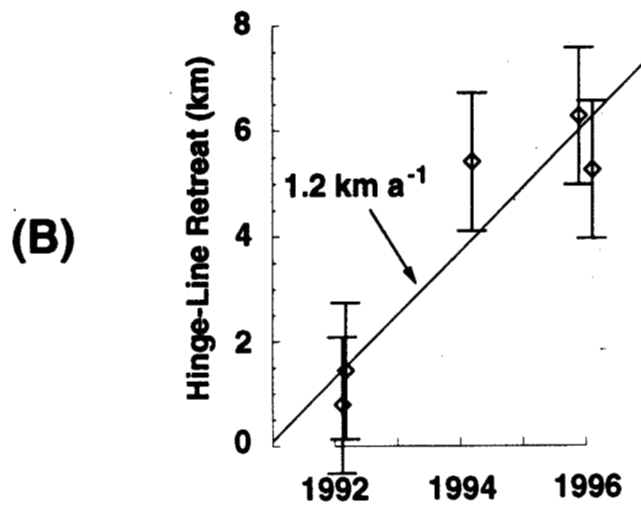
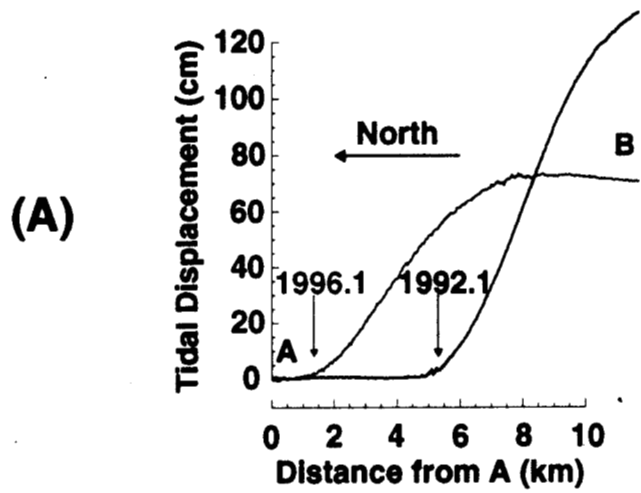


Fig. 2, Rignot